FERMILAB-PROPOSAL-0828 828

Sept. 26, 1990

Letter of Intent to Measure CP Violation in B Meson Decay at the Fermilab Collider

M. Artuso*, R. Kennett-Fox, M. Goldberg, T. Haupt, N. Horwitz, V. Jain, G. Moneti, Y. Rozen, P.D. Rubin, T. Skwarnicki, M. Thulasidas, S. Stone*† W.-Y. Yao, and G. Zhu
Syracuse University, Syracuse, N.Y., 13244-1130

M. Campbell
University of Michigan, Ann Arbor, Mich., 48109

J. Butler, and T. Nash
Fermi National Accelerator Laboratory, Batavia, Ill. 60510

I. INTRODUCTION

We outline here ideas which we envision leading to a proposal for a facility for B physics at the Fermilab Collider. We are studying a solenoidal magnetic detector which will detect particles with high efficiency and good momentum resolution in the central rapidity region. We describe the detector below. We will (a) show that production rates are sufficient for a rich program of B physics including measurements of CP violation in the B system, (b) show that trigger strategies exist which should allow data acquisition using current technology and (c) describe studies that will allow us to better ascertain the physics potential outlined here.

---

* *Present address: Wilson Laboratory, Cornell Univ., Ithaca, N.Y. 14853*

† *Indicates contact person*

II. PHYSICS TOPICS

A) CP Violation

So far, the standard model has been enormously successful in explaining most phenomena in high energy physics. An essential feature is that the mechanism of CP violation occurs because the mass eigenstates of the charged -1/3 quarks are mixtures of the base states. This quark mixing is parametrized as the Cabbibo-Kobayshi-Maskawa matrix. It is convenient to display this in the form given by Wolfenstein shown below.

$$CKM = \begin{pmatrix} V_{ud} & V_{us} & V_{ub} \\ V_{cd} & V_{cs} & V_{cb} \\ V_{td} & V_{ts} & V_{tb} \end{pmatrix}$$

$$= \begin{pmatrix} 1-\lambda^2/2 & \lambda & A\lambda^3(\rho - i\eta) \\ -\lambda & 1-\lambda^2/2 & A\lambda^2 \\ A\lambda^3(1-\rho-i\eta) & -A\lambda^2 & 1 \end{pmatrix}$$

The parameter λ is known from strange particle decays to be 0.22 while A is estimated from b lifetime measurements to be close to 1.0. The two remaining parameters have been constrained by measurements from CP violation in K^0 decay, $\overline{B}$ mixing and b→u/b→c. The relationship between the first two of these and the CKM angles contains strong dependences on the top quark mass as well as some theoretical uncertainties and therefore does not serve to pin down predictions of ρ and η. Measurement of CP Violation in the B system can determine ρ and η independent of m_t. To see what quantities can be measured consider the unitarity relationship:

$$V_{ub}^* V_{ud} + V_{cb}^* V_{cd} + V_{tb}^* V_{td} = 0$$

$$V_{ub} - \lambda V_{cb} + V_{td} = 0$$

which leads to the triangle shown in Fig. 1. Each angle depends on a specific process. Examples of modes that can be used to find the different angles are $B^0 \to \pi^+\pi^-$ for ϕ_1, $B_s \to \rho K_S^0$ for ϕ_2, and $B^0 \to \psi K_S^0$ for ϕ_3. Note that these modes are eigenstates of CP. Use of these modes allows for measurements of the ϕ angles without any complications from the need to compute uncertain hadronic matrix elements. Predictions of the magnitude of the ϕ angles have been given by several authors.[1] The predictions of Kim et al. are shown in Fig. 2. These have resulted from a fit to the data on CP violation in K decay, $B\overline{B}$ mixing and V_{ub}. The prediction should only be taken as a guide of what to expect. CP asymmetries on the order of 20% are expected. The discovery of the top quark and measurement of its mass would sharpen these predictions.

Our aim, however, is not simply to measure ρ and η, but in to establish whether or not the standard model can explain CP violation in the B system. We anticipate that failure to accommodate CP violation would lead to insights beyond the standard model. After all, there are so many parameters that the theory is known to be incomplete. For example, the four KM angles, six lepton masses and six quark masses are not predictable.

We now discuss the method of measuring CP violation at a hadron collider. We take as our example the final state $B^0 \to \psi K_S^0$. Both the production cross-section and branching ratio are known (at least approximately). We first need to design a trigger for these events. Two generic types of trigger are conceivable. The first is specific to the final state under study. In this case a good trigger can be made for the ψ. The other type of trigger would be to select any B and then find the ψK_S^0 events in the sample. An example of this would be a high p_t lepton trigger. For now let us assume we have triggered on an adequate sample of events and discuss what we want to measure. The CP asymmetries in B decay

have been described in detail by Bigi and Sanda.[2] In hadron-hadron collisions we must consider three distinct cases.[3] Case (i) has the B^0 produced in conjunction with a $B^{\pm}$ or a B baryon, while in case (ii) the B^0 is produced in conjunction with a $\overline{B}^0$. In case (iii), the B^0 is produced in conjunction with a B_s. Case (i) is the easiest to treat. CP violation can occur because there are two amplitudes present which can interfere. One is the direct decay of $B^0 \rightarrow \psi K_S^0$ while the other has the B^0 mix to a $\overline{B}^0$ which then decays to ψK_S^0. CP violation becomes observable in the difference in rates between $(\psi K_S^0, B^+)$ and $(\psi K_S^0, B^-)$. The time dependence is explicitly given by:

$$Rate[\psi K_S^0\,(t)\,, B^+] \;\propto exp\{-\Gamma t\} \times \{1 - sin\,(\Delta m t)\, sin\, 2\phi_3\}, \tag{1}$$

While for a B^- the sign in front of the sine term flips:

$$Rate[\psi K_S^0\,(t)\,, B^-] \;\propto exp\{-\Gamma t\} \times \{1 + sin\,(\Delta m t)\, sin\, 2\phi_3\}. \tag{2}$$

Both Γ, which is $1/\tau_b$, and Δm have been measured. (Δm/Γ is found to be 0.73 from $B^0\overline{B}^0$ mixing.) These two rates are shown as a function of time in Fig. 3a. For illustrative purposes we have taken the case of $sin\, 2\phi_3 = 0.4$. The central curve is a simple exponential. CP violation is manifest in the difference between the two rates defined in equations (1) and (2). It can be expressed in terms of the asymmetry, defined as the difference of the two rates divided by their sum:

$$ASY(t) = sin\,(\Delta m t)\, sin\, 2\phi_3. \tag{3}$$

$ASY(t)$ is shown in Fig. 3b. It should be noted that time dependent measurements are not necessary, in principle, to find the CP violating asymmetry, although vertex detection is crucial in rejecting backgrounds and thus the proper time of the decay

of the ψK_S^0 will be well available. Thus a fit to the predicted time distribution can be used to reduce backgrounds and understand systematics. The time integrated asymmetry is equal to $\left(\frac{x}{1+x^2}\right) sin\, 2\phi_3$, where $x = x_d = \Delta m/\Gamma$.

The next case that we need to consider is that of ψK_S^0,B^0. Several complications arise here because both neutral B's can mix. Furthermore, we must consider separately both C=$\pm$1 initial $B^0\overline{B}^0$ states and then average them. We have:

$$Rate[\psi K_S^0\,(t)\, B^0\,(t')\,]_{C\mp} \propto exp\{-\Gamma\,(t+t')\}\times\{1\mp sin\,[\Delta m\,(t\mp t')]\; sin\, 2\phi_3\}. \quad (4)$$

Integrating over t' and averaging over C=$\pm$ states, we find

$$Rate[\psi K_S^0\,(t)\,, l^+] \;\propto exp\{-\Gamma t\}\times\{1+\left(\frac{1}{1+x^2}\right) sin\,(\Delta m t)\; sin\, 2\phi_3\}. \quad (5)$$

While for an l^- the sign in front of the sine term flips:

$$Rate[\psi K_S^0\,(t)\,, l^-] \;\propto exp\{-\Gamma t\}\times\{1-\left(\frac{1}{1+x^2}\right) sin\,(\Delta m t)\; sin\, 2\phi_3\}. \quad (6)$$

The time dependence is the same as in the charged B case, but the asymmetry is reduced by a factor $\left(\frac{1}{1+x^2}\right)$ equal to 0.65.

The third case containing a ψK_S^0 along with a B_s is easily dealt with by noting that the CP asymmetry is reduced by a factor $\left(\frac{x_s}{1+x_s^2}\right)$. Since x_s is expected to be at least a factor of six larger than x_d, the CP violating contribution from this source is negligible. It is expected that lower limits on x_s will be found by other experiments or this experiment (see below for a discussion of B_s mixing).

What we propose to measure is the time dependent asymmetry found by detecting ψK_S^0 along with a tag of the flavor of the other B. At this time it appears

that the best choice of this tag is lepton (either electron or muon). Thus the measured quantity is:

$$ASY(t) = \left(\frac{\sigma\left(\psi K_S^0(t), l^-\right) - \sigma\left(\psi K_S^0(t), l^+\right)}{\sigma\left(\psi K_S^0(t), l^-\right) + \sigma\left(\psi K_S^0(t), l^+\right)} \right). \tag{7}$$

To extract the quantity $sin\, 2\phi_3$, as given in equation (3), we need to average over the number of events in each of the three cases described above. To first order this is given by the ratio of the inclusive rates of B^0, B^-, B_s and Λ_b. Since relative branching ratios of B^0 and B^- are known and those for B_s can be estimated, we can measure the relative fractions of these mesons by detecting them. The only remaining problem is how many Λ_b's there are. These can be estimated by Monte-Carlo and will contribute a small systematic error to the measured value of $sin\, 2\phi_3$.

Although we have given a particular example of one decay mode that can be used to measure CP violation we will be interested in using other modes. A Table of other potentially interesting modes is given in the Appendix. Particular interest exists in measurements of modes such as $B^0 \to \pi^+\pi^-$ and $B_s \to \rho K_S^0$ because they probe the other angles. However, detailed estimates of the feasibility of detecting these modes awaits measurement of their branching ratios.

B) B_s Mixing

Another constraint on the KM angles, and thus an independent test of the standard model, can be found from a measurement of B_s mixing. Although the magnitude of $x_s = (\Delta m/\Gamma)_s$, depends on the top quark mass, the ratio of B_s to B_d mixing is independent of m_t. We have:

$$\frac{x_s}{x_d} = \frac{B_{B_s}}{B_{B_d}} \cdot \frac{f_{B_s}^2}{f_{B_d}^2} \cdot \frac{|V_{ts}|^2}{|V_{td}|^2} = \frac{1}{\lambda\left[(1-\rho)^2 + \eta^2\right]}. \tag{8}$$

The ratio of "bag factors," B_B, and decay constants, f_B, must be derived from theory. However, the ratios are expected to be close to unity. Thus we would have a relatively precise constraint on the two parameters ρ and η which could be compared with other constraints such as the one from b→u or CP violation.

We now discuss how we would go about measuring x_s. In the standard model B_s mixing is expected to be at least six times larger than B_d mixing. This means that the method used to find B_d mixing, namely measuring the number of like sign dileptons with respect to the number of opposite sign dileptons, will yield only a lower limit on the size of x_s. To measure this quantity we need to measure the time dependence of the B_s decay. For a B_s to decay as a B_s the time dependence is given by $e^{(-\Gamma t)} cos^2 \left(\frac{\Delta m}{2}\right) t$, while for a B_s to decay as a $\overline{B}_s$ the time dependence is given by $e^{(-\Gamma t)} sin^2 \left(\frac{\Delta m}{2}\right) t$. The time dependence for B_s to decay as a B_s is shown in Fig. 4a, for a $\Delta m/\Gamma$ of 7.3.

To measure this time dependence it is necessary to tag the flavor of B_s at its birth and also know its flavor when it decays. We propose to do this by fully reconstructing some B_s decays and using a lepton from the other B to tag the birth flavor. Some decay modes that are useful for this purpose include $D_s^+\pi^-$, $D_s^{*+}\pi^-$, $D_s^+\rho^-$, and $D_s^{*+}\rho^-$. Note, that modes containing $\psi's$ are not useful for this purpose, since it is impossible to tell if the mode is a decay of a B_s or a $\overline{B}_s$. (Of course these modes can be used to check if CP violation is as small here as predicted.) Again, as in the measurement of CP violation, we must consider three different situations depending on what kind of B is produced along with the B_s. In the first case the other B is charged or a B baryon. This case gives the time dependence mentioned above. In the second case the other B is a B^0 (or a $\overline{B}^0$). Here we must correct for the possibility of the other B mixing as well. Fortunately, the mixing rate is only 20% In the third case a $\overline{B}_s$ is produced. Now both B's can

oscillate into each other. The resultant signal is reduced by these effects as shown in Fig. 4b. x_s is measured by a fit to the data which determines the oscillation period.

C) Rare and Ultra-Rare B Decays

In this section we discuss decays that both are expected and unexpected in the standard model. One class is "Penguin" Decays. These decays occur in one loop diagrams in the standard model. This mechanism is thought to explain the ΔI=1/2 rule in kaon decays but no examples of explicit Penguin decays can be seen in the kaon sector. In the B sector the decay thought to be the easiest to observe is $K^*\gamma$. Other decays include Kl^+l^- and hadronic decays such as $K\pi^\pm$. The predicted branching ratios for these decays are in the range of 10^{-5} to 10^{-4}. Current upper limits are near the top end of this range.

Other decays which could reveal new physics include $\mu^+\mu^-$ expected at a very low rate of 10^{-8} in the standard model, and the lepton violating μe mode. Although unlikely to occur, these modes are important to search for to test the completeness of the standard model.

D) Spectroscopy: The B_c and B Baryons

Although inherently less interesting then direct tests of the standard model, the spectroscopy of the B system is best investigated at a hadron machine where the B_c and Λ_b's are produced at the same time studies of other phenomena are occurring. The B_c will decay prolifically to ψ's while Λ_b's will have large decay rates to Λ_c.

III. THE DETECTOR

A) Introduction

It is our intention to build upon the recent success of CDF in seeing some fully reconstructed B mesons. Therefore we would like to work in the central rapidity region where data exist on particle yields. Furthermore, the detector elements need to be well matched to the triggering and data acquisition schemes. We need to plan on accumulating on the order of 10^8 B's per year to measure CP violation in the B system and attack the other B physics questions mentioned above. Since we have $\approx 10^7$ seconds in a year we must accommodate a real trigger rate of 10 Hz and must allow for a rate of at least 100 Hz, to allow for background triggers and luminosity increases. We envision a "pipeline" type system where we have enough computing power online to select good events and write them to tape.

Conceptually the detector divides at the magnet coil. Outside the coil we need have only muon detection and the capability of triggering on muons and dimuons. The current hardware structure of CDF, for example, appears to be appropriate. Inside the coil we need detection elements that are more specific to B physics. A precision vertex detector is necessary to reduce backgrounds in the B sample and to measure the time dependencies for B_s and mixing and CP violation. It would be very useful if this detector measured both r-ϕ and r-z coordinates. Outside the vertex detector is a precision drift chamber capable of measuring charged particle momenta to high accuracy. The design must be such that the mass resolution on reconstructed B's is 20 MeV (r.m.s.) or better. Surrounding the drift chamber is an array of crystals. These crystals could be made of pure CsI, BaF_2 or even PbF_2. The choice would be based on their cost and the sensitivity to radiation. A sketch of the inner part of the detector is shown on Fig. 5. Next we describe the apparatus in more detail.

B) Vertex Detector

A high precision vertex detector plays a crucial role in the proposed experiment. In order to study CP violation in B decays it is necessary to reconstruct an exclusive CP eigenstate coming from neutral B decay, like ψK_s, with good efficiency and minimal background contamination and to tag the flavor of the decaying $\overline{B}$. A large fraction of the background, produced by chance combination of tracks, can be rejected by requiring that the decay products originates from a common vertex displaced with respect to the primary event vertex. In addition, the capability of identifying secondary vertices with good spatial resolution is a fundamental requirement for efficient flavor tagging of the CP eigenstate. For example, the simplest and best known way of tagging uses the charge of the lepton coming from B semileptonic decay. Backgrounds are reduced if the leptons are required not to intersect the main vertex. Furthermore, if the subsequent D decay vertex is isolated, then a wider range of lepton momenta can be used without being concerned about the contamination coming from cascade decays of the kind $B \rightarrow D\ Y$ with $D \rightarrow l\nu X$, which would produce a wrong sign tag and therefore would dilute a possible effect. In addition new approaches to flavor tagging are going to be investigated, such as using the charge balance at displaced vertices. Some of these techniques may produce a sizable reduction in the luminosity required to perform a significant measurement of CP asymmetry in B decays.

Fig. 6a shows the expected spatial distribution of B meson decay vertices and Fig. 6b the spatial distribution of the separation between B vertex and daughter D vertex according to a Monte Carlo simulation performed using the ISAJET event generator. The D decay displacement has been plotted for three different values of the lower cut off of parent B momentum and it can be seen that the spatial distribution is only weakly dependent upon this parameter. An efficient separation

of the B and D vertices requires a state of the art vertex detector. For example, in order to have an efficiency of 80% in separating B from D vertices a separation of the order of 100 μm must be adequately measured, requiring a device with a spatial resolution of the order of 30–50 μm rms.

Several different approaches can be adopted in designing a high precision vertex detector. It should be stressed that the field of high precision position sensitive devices is presently the object of very active and exciting R& D studies from which our final design will certainly benefit. The final design will require an optimization of the technology adopted for the various layers and the corresponding segmentation in order to achieve the most effective pattern recognition capability consistent with adequate spatial resolution. A combination of double sided silicon strip detectors and pixel devices can be a very promising solution. Figures 7 and 8 show the transversal and longitudinal impact parameter resolution of two possible configurations involving either three layers of pixel devices equally spaced in a radial distance between ranging between 3 and 7 cm., or one layer of double sided silicon 300 μm thick and two layers of pixel devices. The radial range is consistent with the present design of the silicon inner tracking system to be installed in the CDF detector. The beam pipe assumed is 500 μm thick beryllium at 2.5 cm radius. The possibility of reducing this radius should be pursued as it would improve spatial resolution. The pixel detectors are assumed to have an individual thickness of 500 μm, which seems to be a reasonable assumption consistent with present technology. The double sided inner layer has a thickness of 300 μm. The number of layers has been kept to a minimum to avoid spoiling the intrinsic resolution of the silicon devices; the addition of sizable amount of material would limit the efficiency of the vertex detector and have a negative effect on other parts of the detector like central tracking and electromagnetic calorimeter. This design philosophy requires

two dimensional devices to enable efficient pattern recognition. A combination of an inner layer with strips and outer layers with pixel devices seems the optimum solution as far as resolution is concerned. We need to study how to implement this solution for a detector length of 50 cm required due to the longitudinal spread of the interaction point. The number of processing channels for the longitudinal strips required to achieve the spatial resolution assumed would be of the order of 10000 per side of the polygonal structure surrounding the beam pipe. This large number gives serious problems in cooling the VLSI electronics and capability of locating it outside the active solid angle of the detector. Thus, reducing the size of the interaction region would be useful. (Recent studies by Gerry Dugan have shown that this spread can be reduced to below 10 cm. Implementing this change would be extremely useful.)

An additional remark which is pertinent to the fast trigger design is that a silicon tracker is a very efficient alternative to an inner gas chamber for triggering purposes. The charge collection in a fully depleted device takes at most a few nanoseconds and the only time limitation comes from the processing electronics. Intelligent processors which allow quick sparsification of the signals and readily available latched hit information are presently the object of widespread study and development and are likely to be available in the next few years.

C) Drift Chamber

The main tracking chamber must reconstruct B mesons with high efficiency and good mass resolution, have information available for the trigger, and be useful for identifying electrons and kaons using ionization loss. This chamber when coupled with a precision vertex detector (described elsewhere) will locate the decay vertices and reduce combinatorial backgrounds using clean projected tracks from

the main tracking chamber. While good spatial resolution is the key to measuring high transverse momentum tracks, multiple scattering in the tracking chambers dominates the resolution of low momentum ones. Similarly, photon reconstruction efficiency in the calorimeter decreases with absorption in dead material.

In order then, to achieve our experimental goal of identifying large numbers of B mesons, with a mass resolution of no worse than 20 MeV, we require a drift chamber system with minimizes multiple scattering, uniformly covers a large solid angle, discriminates particle types via pulseheight measurements, and provides for track pattern recognition at the trigger level as well as offline. These requirements can be met with a system that covers the full r and z dimensions between the vertex detector and the electromagnetic calorimeter, utilizes a low density, low diffusion gas mixture and low mass wire and endplate materials. Due to the length of the chamber we must be careful in obtaining an inherently stable electrostatic configuration. We believe that a design like the small-cell one of the CLEO II drift chamber, but employing state-of-the-art components, will be adequate. We envision, however, a possible two-chamber solution: an inner chamber providing within a microsecond r-z and momentum measurments reliable enough to associate with signals from the lepton detectors at the first level trigger; and a main drift chamber providing r-ϕ information for crude track pattern recognition to associate with the vertex detector and inner chamber at the second level trigger. Gross calibrations of the two chambers should reduce position and drift-time relations uncertainties to a degree sufficient for fast online track fitting and projecting to the calorimeter and iron, thereby allowing for high momentum lepton identification in the trigger. Offline, when thoroughly calibrated, the drift chamber porvides precision track fitting giving the desired momentum resolution and information necessary to find secondary vertices and perhaps to locate decays-in-flight.

We intend to perform Monte Carlo calculations to determine the viability of this scheme in an environment of backgrounds and realistic occupancy rates.

D) Crystal Detector

The crystal detector has several functions. In is situated inside the coil so that it will have excellent resolution on low energy photons. One reason for this is that the process $B^* \rightarrow \gamma B$ can be very useful for reducing backgrounds in some B decay modes. This is similar to the trick used in studies of D physics where the process $D^{*+} \rightarrow \pi^+ D^0$ has been used to substantially reduce backgrounds in D^0 signals. Since the Q value in the B^* transition is only 50 MeV, the energy resolution measurement must be good for these low energy photons.

Another use is to find decay products of B's that decay into neutrals. This is particularly important for the measurement of B_s mixing where the decay modes contain a D_s^+ or a D_s^{*+}. Since the only decay mode is $D_s^* \rightarrow \gamma D_s$, detecting low energy photons is essential. It is also very useful in detecting D_s decay since the mode with the largest hadronic branching ratio in D_s^+ decay is $\eta' \pi^+$. Furthermore, it is clearly useful to be able to detect $\rho^\pm$ which arise from the decay of the virtual W in association with the D_s or D_s^*.

The measurement of CP violation is also enhanced by having the crystals because modes such as $B^0 \rightarrow \psi K^{*0}, K^{*0} \rightarrow K_S^0 \pi^0$ and $B^0 \rightarrow \rho^\pm \pi^\pm$ become measurable.

Our tentative design has the crystals 16 radiation lengths thick and about 5cm x 5cm in cross section. The crystals would point to the interaction region. Thicker crystals would improve the energy resolution above 5 GeV but would be more costly both in terms of dollars and in terms of space. The method of light detection is currently under investigation at Syracuse. Photodiodes have

been successfully used in magnetic fields, and at large scale with Thallium doped CsI crystals. The light yield are lower in the materials we need to withstand radiation damage. The devices we are considering have gains in excess of ten. One promising device uses a photocathode and a silicon photodiode with a 10KV potential between them. This device, invented by Riccardo DeSalvo of CERN can have gains of up to 1000 and should be inherently stable. We are also investigating the radiation hardness of pure CsI in full size prototype crystals.

IV. B PRODUCTION RATES AND TRIGGER SCHEMES

A) Trigger Schemes

In general there are two possible trigger scenarios. In the first, one triggers on a decay product of the B that is to be fully reconstructed. For example a ψ from $B^0 \rightarrow \psi K_S^0$ decays. In the second case, one triggers on a generic B decay product. For example, a high P_t lepton. We propose to implement both types of trigger schemes in order to maximize the number of physics topics.

The J/ψ trigger will look for either the di-electron or di-muon decay mode of the J/ψ. The dimuon trigger will require both muons above the range-out momentum, which in the case of a muon system like CDF would be around 3 GeV. This trigger would have a cross section of about 0.05 microbarns, corresponding to a rate of about 5 Hertz at a luminosity of 10^{32}. There will be a crude ϕ match between a muon stub in the muon chambers and the central tracking system required in order to achieve this low cross-section.

The dielectron trigger for the J/ψ will require two electromagnetic clusters with two matching tracks in the central region. It is more difficult to estimate the cross section for this trigger without detailed simulation of the detector and

the trigger system. Studies that are currently under way for the CDF detector indicate that a cross section of about 1 microbarn can be achieved for single 4 GeV electrons from B decay, so it is expected that the rate from the dielectron trigger will be small.

The single electron trigger and single muon trigger will be used for tagging one of the B decays through the semileptonic decay mode. The single muon trigger for CDF is set at 9 GeV P_t, and the cross section is about 1.1 microbarns. The upgraded muon system is expected to push this rate down by about a factor of 20 in the central region.

The single electron trigger will be based on identifying an isolated electromagnetic cluster in the crystals and matching the energy of the cluster to the momentum of a track from the central region. Recent simulations in the CDF detector, using sophisticated pattern recognition hardware from INTEL, indicate that a factor of two can be gained by looking at the surrounding calorimeter cells and requiring that they be consistent with a B decay. With the crystals having a much finer segmentation than the CDF detector which was used in this study it is likely that another factor of two can be gained. These advantages can of course be offset if the amount of material in the tracking system adds to more than a few percent of a radiation length. The expected cross section for this trigger at 4 GeV E_t is about 1 microbarn, giving a rate of 100 Hertz at 10^{32} lumiinosity.

These triggers are based on electrons and muons; there is a tremendous amount of experience on finding signatures for the leptons. It would be difficult to do any further reconstruction of the event in the trigger without having 3-D tracking in hardware. Track finding in only the r-ϕ plane restricts the invariant mass reconstruction to use only transverse mass. Studies of doing this kind of reconstruction in the context of J/ψ in the CDF detector showed that there was very little to be

gained. In any case, since the crystals are projective, the θ angle is measured and this allows an actual mass to be calculated for the electron case.

The total trigger rates from this set of triggers will be about 200 Hertz at a luminosity of 10^{32}. The CDF detector for 1993 will have a data acquisition system able to accommodate 100 Hertz, so it is expected that 200 Hertz will not be pushing the state of the art.

B) Production Rates

Cross sections for B production have been calculated to order α_s^3 by Ellis, Nason and Dawson.[4] The cross section in 1.8 TeV $p\bar{p}$ collisions for $|\Delta y| < 1$ as a function of the minimum P_t of the B is shown in Fig. 9. Above a P_t of 5 GeV/c the cross section over ± 2 units of y is $15\mu b$ It is our contention that these cross sections are at least approximately correct because the same calculations at 630 GeV agree with the UA1 data. The comparison with UA1 is shown in Fig. 10. It would be useful here to have cross section measurements from CDF using their recent oberservations of B decays.

Of more interest to the measurements we seek to perform is the cross section for having a lepton from one B and the decay products of the other B in the region of good acceptance. Some important considerations are: (1) the detector will have good acceptance and resolution in the region $|\Delta y| < 2$; (2) the vertex separation of the B from the collision point becomes worse as P_t decreases. For a P_t of 2.5 GeV/c, $\gamma\beta \approx 1/2$ and the B decay has a mean path perpendicular to the beam direction of $180\mu m$, allowing for relatively easy detection; (3) triggering on a lepton with $P_t > 4$ GeV/c is relatively easy but becomes more difficult quickly for lower P_t. We have done a Monte-Carlo calculation of the cross-sections of interest using ISAJET to give us correlations. The α_s^3 corrections have been included. We

have normalized the single B cross sections to the values of Nason et al.

We now display the cross sections for having a decay lepton from one B and all the decay products of the other B when it decays into ψK_S^0 (used as an example) in the region of $|\Delta y|$ <2, as a function of P_t of the lepton and P_t of the B in Fig. 11. The contour lines show the integrated cross sections for having both one B with P_t greater than the amount shown on the vertical axis and the other B decaying into a lepton with P_t greater than the amount shown on the horizontal axis. All the branching ratios in the ψK_S^0 decay have been accounted for. If we choose, for example, the contour showing 10pb cross-section, a 100pb^{-1} run would give us 1000 fully reconstructed and flavor tagged events. One choice on the 10pb curve has the P_t of the lepton be greater than 5 GeV/c and the P_t of the B also be greater than 5 GeV/c.[5] It may be that the proper variable in which to view these rates is the momentum P of the lepton rather than P_t. In Fig. 12 we show the cross-section contours for P of the lepton versus P_t of the ψK_S^0. In this case we have a 10pb cross-section when the lepton momentum is greater than 7 GeV/c and the ψK_S^0 P_t is greater than 5 GeV/c.

The number of events needed to measure $sin\, 2\phi_3$ to a significance of S standard deviations is given by

$$N = \left(\frac{S}{d \cdot sin\, 2\phi_3}\right)^2 . \tag{9}$$

The factor d is a dilution factor which is determined by the mixture of charged (1.0), neutral (0.65) and strange (0) B's. We estimate this factor to be 0.76. Then 1000 fully reconstructed and tagged ψK_S^0 events allow us to establish CP violation at the four standard deviation level if $sin\, 2\phi_3$ is a low as 0.17. Lower values can be reached by taking more data, goes as square of luminosity, using more decay modes such as $\psi K_S^0, K_S^0 \rightarrow \pi^0\pi^0$ or $\psi K_S^0 \pi^0$, or increasing the flavor tagging efficiency.

However, we must beware that wrong sign tags are costly. They introduce an additional dilution in the required luminosity by a factor of $(1-2w)^2$, where w is the wrong sign fraction.

We now comment on different strategies for tagging the B flavor. This is most pertinent in the situation where we have triggered on a ψ and need to tag the flavor of the other B. We have thus far discussed using only a high P_t lepton, which we have assumed to be background free. Other methods are possible and we are investigating them. They include: using charged kaons as a tag, counting the charged multiplicity in the tag vertex and looking for a secondary vertex having either a D^+ or D^- which would also be a flavor tag. We have also found that using the highest momentum charged track from a B decay provides a useful tag. Preliminary estimates give an approximately 30% efficiency with only 15% of these being wrong sign. Any of these methods serve to enhance the useful cross section. We make no claims at this point on how much tagging efficiency we can gain with these stratagems. However, we point out that whatever strategy we care to try we can evaluate eventually using real data. The $\psi K^{\pm}$ and $\psi K^{\pm}\pi^{\mp}$ are each about a factor of two more prolific than the CP eigenstate modes and we could use these modes as a laboratory to evaluate the tagging efficiencies and backgrounds.

These strategies for tagging need to be simulated. We need to ascertain the smallest value of lepton P_t that can be used for triggering or tagging and the triggering efficiencies on leptons from J/ψ decay as a function of the B momentum. We also would like to see how the precision of the CP measurement varies as the P_t of the B decreases. We may be able to substanially improve the useful cross-section above the 10pb level chosen above.

V. FUTURE ACTIVITIES

We believe that the measurement of CP violation in the B system is important and that it probably can be done at the Fermilab Collider. The concepts presented in this letter need to be expanded upon and detailed designs need to be implemented in order to make this a full proposal. It setting forth these ideas we ask the laboratory to enter into discussions in order to ascertain the laboratory's interest, the possibilities of doing this experiment at a collider intersection region, and what support the laboratory could provide. Thus far we have not attempted to enlist a large number of collaborators, preferring to set out the initial concepts with a small number of interested people. If the laboratory is interested in pursuing this direction, we would now like to enlarge the group.

References and Footnotes

1) C .S. Kim, J. L. Rosner and C. P. Yuan, Univ. of Chicago Preprint Efi-89-47 (1989); C. O. Dib, I. Dunietz, F. J. Gilman and Y. Nir *Phys. Rev.* **D41,** 1522 (1990) .

2) I.I. Bigi and A.I. Sanda *Nucl. Phys.* **B281,** 41 (1987) .

3) I. Dunietz and J. L. Rosner *Phys. Rev.* **D34,** 1404 (1986) .

4) P. Nason, S. Dawson and R. K. Ellis *Nucl. Phys.* **B327,** 49 (1989) .

5) The actual efficiency of detecting a B will depend on the specific decay mode of interest. We expect that the hardware will be sufficiently robust that a track which is in the $|\Delta y| < 2$ region will be detected.

APPENDIX - CP Eigenstates

Useful Modes for Measuring CP Violation			
Mode	Branching Ratio	Accessible BR†	Relative to ψK_S^0
ψK_S^0	4.0x10^{-4}	5.6x10^{-5}	1.0
$\psi' K_S^0$	$\leq$3.0x10^{-4}	$\leq$1.4x10^{-5}	$\leq$0.3
$\psi K^{*0}, K^{*0} \rightarrow K_S^0 \pi^0$ (A)	2.5x10^{-4}	3.5x10^{-5}	0.4
$D^+ D^-$	1.2x10^{-3}	2.7x10^{-5}	0.5
$D^{*+} D^- + D^+ D^{*-}$ (B)	3.0x10^{-3}	6.2x10^{-5}	1.1
$D^{*+} D^{*-} (A)$	4.0x10^{-3}	7.6x10^{-5}	1.4
$D^0 \pi^0 + D^0 \rho^0 + D^{*0} \rho^0$ (C)	3.5x10^{-3}	5.6x10^{-5}	1.0
With unknown branching ratios			
$\chi K_S^0 or \chi K^{*0}$			
$\pi^+ \pi^-$			
$\rho^{\pm} \pi^{\mp}$ (D)			
$B_s \rightarrow \rho^0 K_S^0$			
$B_s \rightarrow \rho^0 K^{*0}, K^{*0} \rightarrow K_S^0 \pi^0$ (A)			

† Includes branching ratio of ψ, ψ' or D to accesible low multiplicity modes

(A) Can be used by studing angular distribution of K^{*0}decay

(B) $sin\, \phi_3$ can be unraveled from measuring both modes with both sign tags

(C) where $D^0 \rightarrow$CP Eigenstate

(D) $sin\, \phi_2$ can be unraveled from measuring both modes with both sign tags

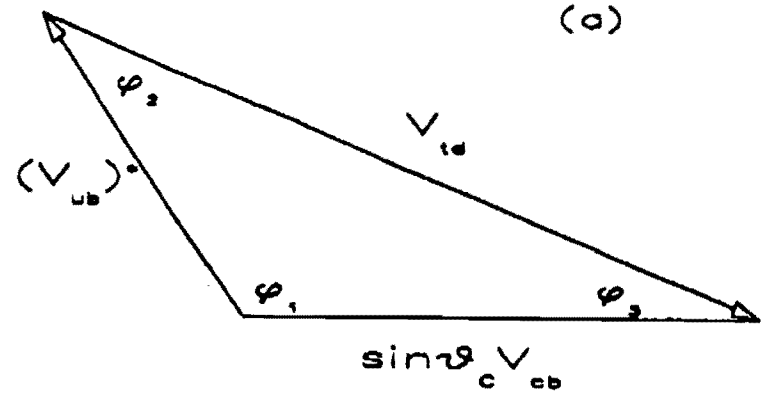
(a)
φ_2
V_{td}
$(V_{ub})^*$
φ_1
φ_3
$\sin\vartheta_c V_{cb}$

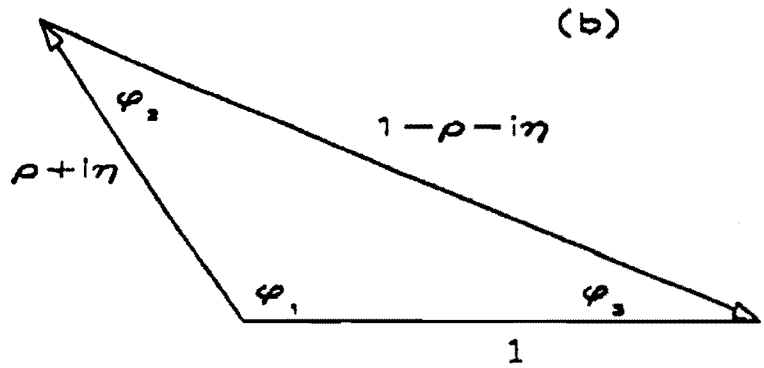
(b)
φ_2
$1-\rho-i\eta$
$\rho+i\eta$
φ_1
φ_3
1

FIGURE 1

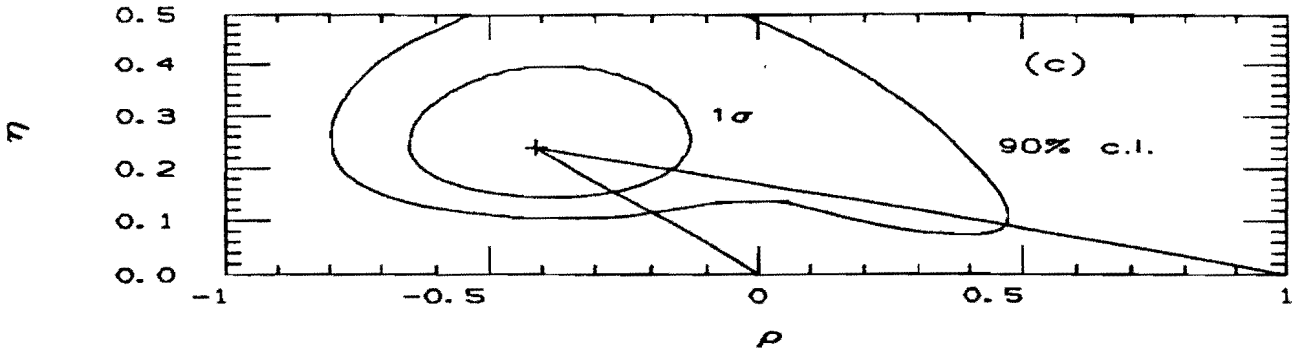

Figure 2

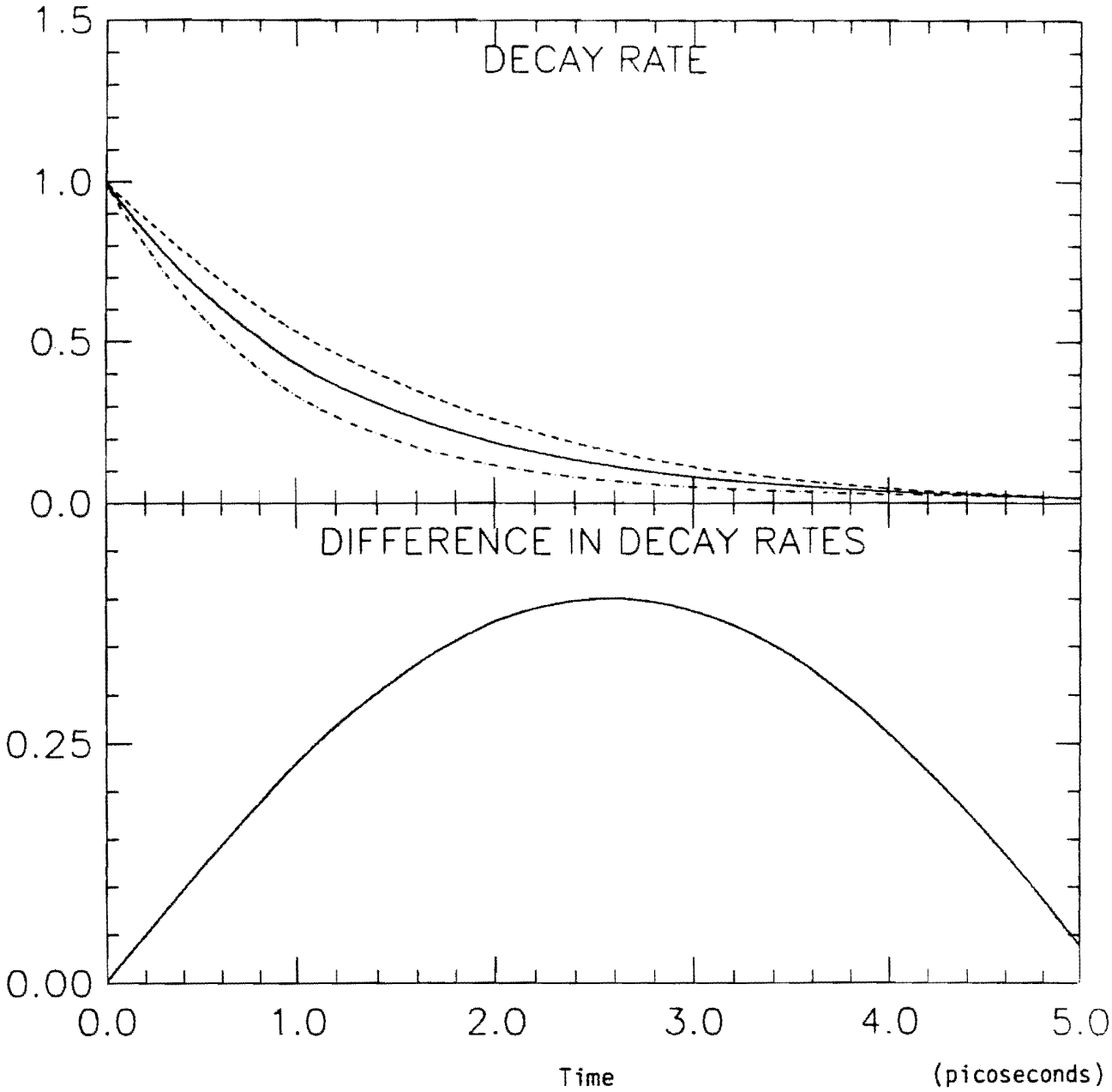
DECAY RATE
1.5
1.0
0.5
0.0
DIFFERENCE IN DECAY RATES
0.25
0.00
0.0
1.0
2.0
3.0
4.0
5.0
Time
(picoseconds)

Figure 3

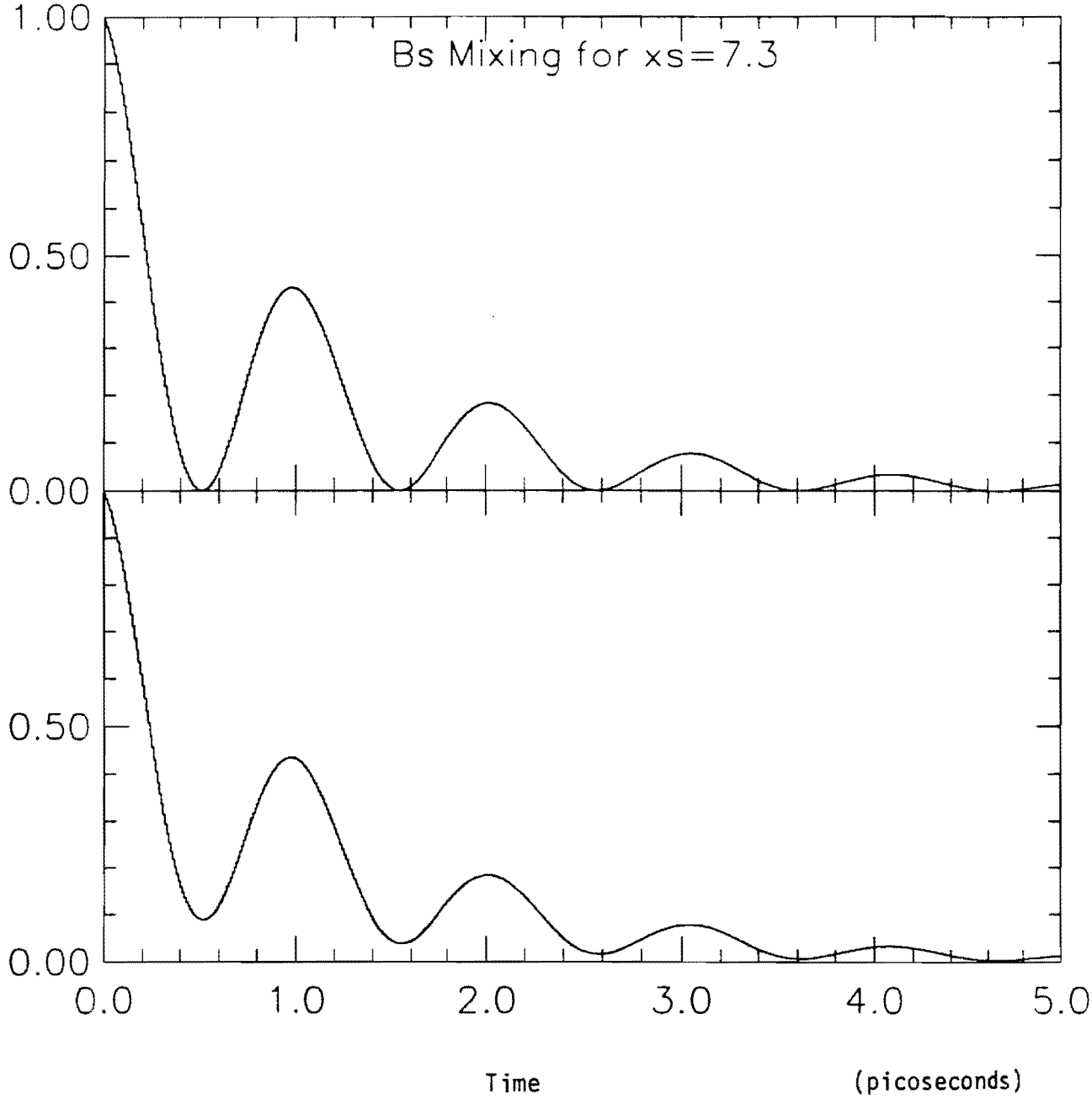
Bs Mixing for xs=7.3
1.00
0.50
0.00
0.50
0.00
0.0
1.0
2.0
3.0
4.0
5.0
Time
(picoseconds)

Figure 4

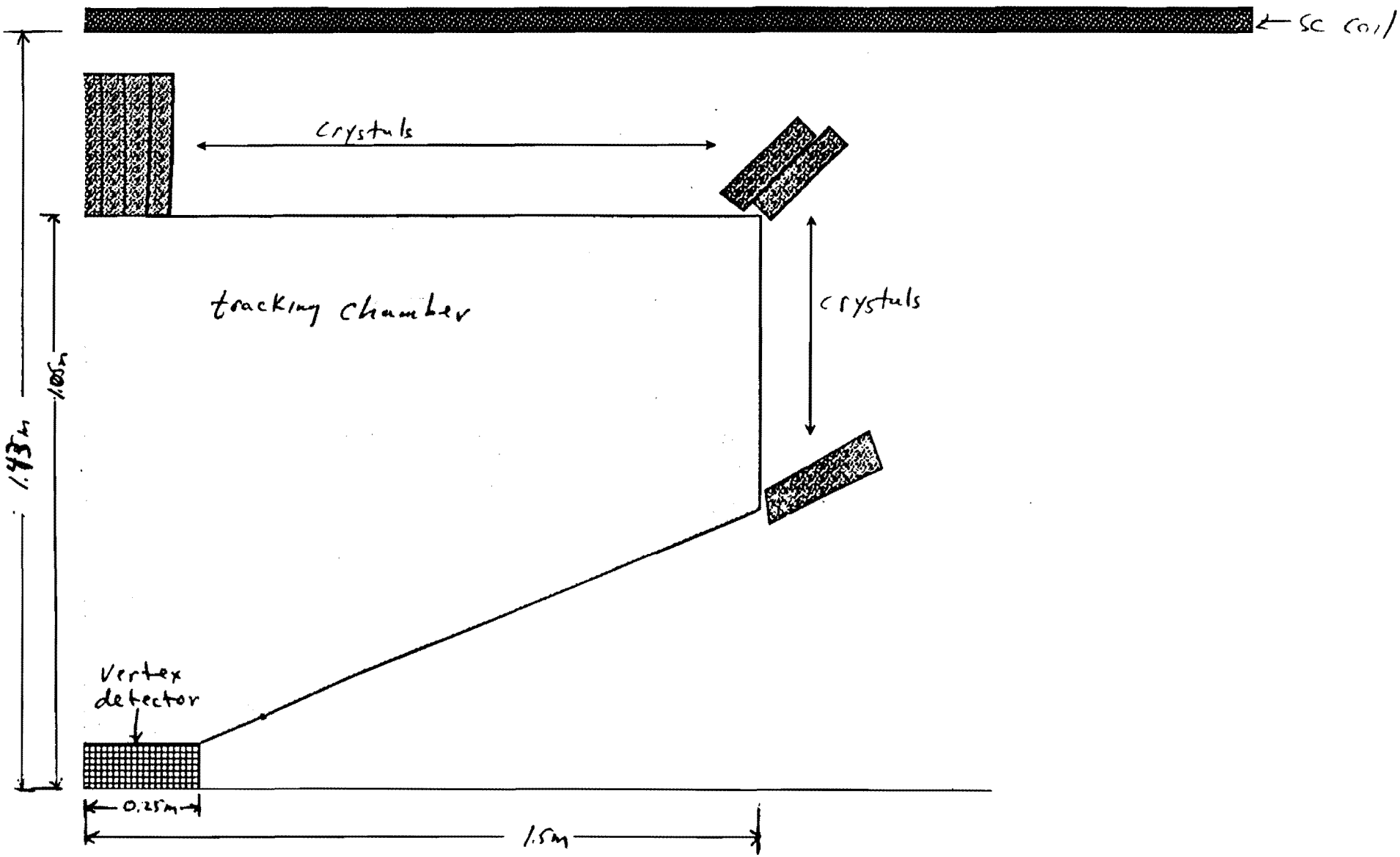
SC coil
crystals
tracking chamber
crystals
1.43m
50%
Vertex detector
0.25m
1.5m

Figure 5

Figure 6: a) B meson decay vertex separation from the primary vertex. b) D meson decay vertex separation from the parent B decay point. Continuous line corresponds to decay products of B mesons with momentum greater than 1GeV, dashed line to decay products of B mesons with momentum greater than 5 GeV, dotted line to decay products of B mesons with momentum greater than 10 GeV.

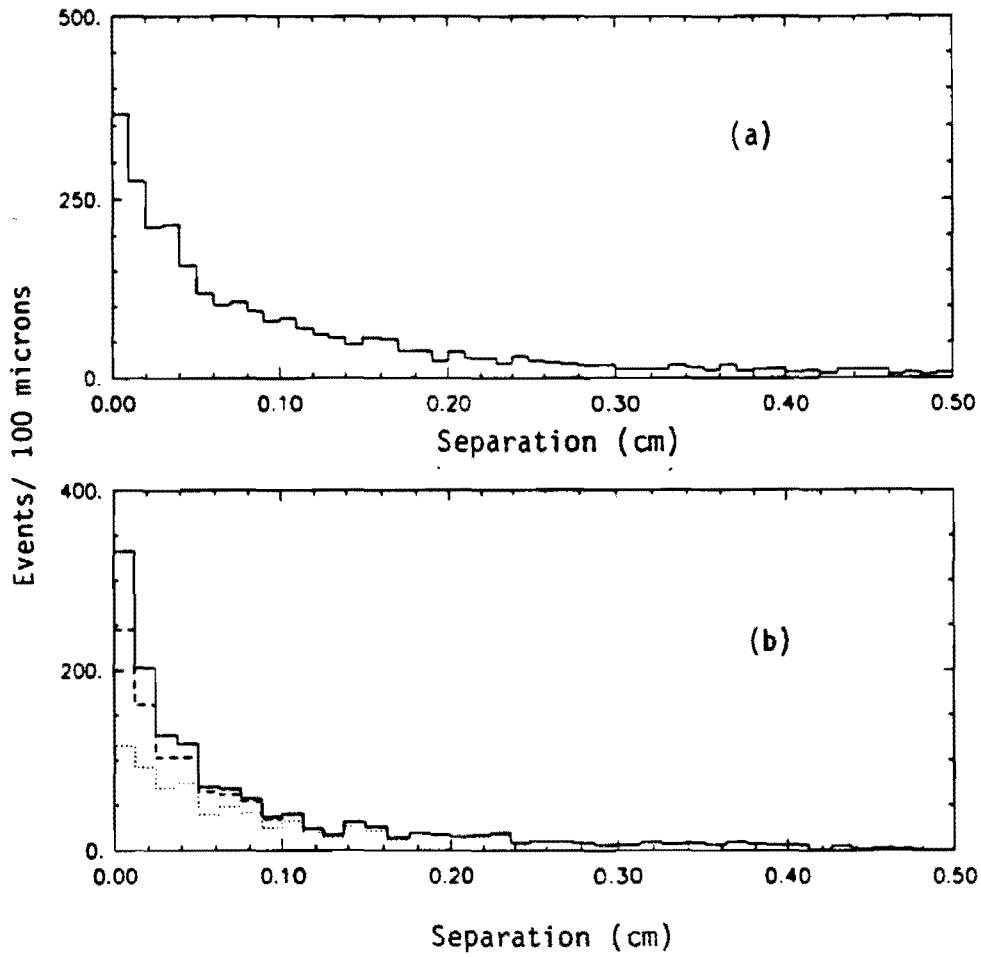

Figure 7: Impact parameter resolution of 3 layer pixel detector as a function of the dip angle.

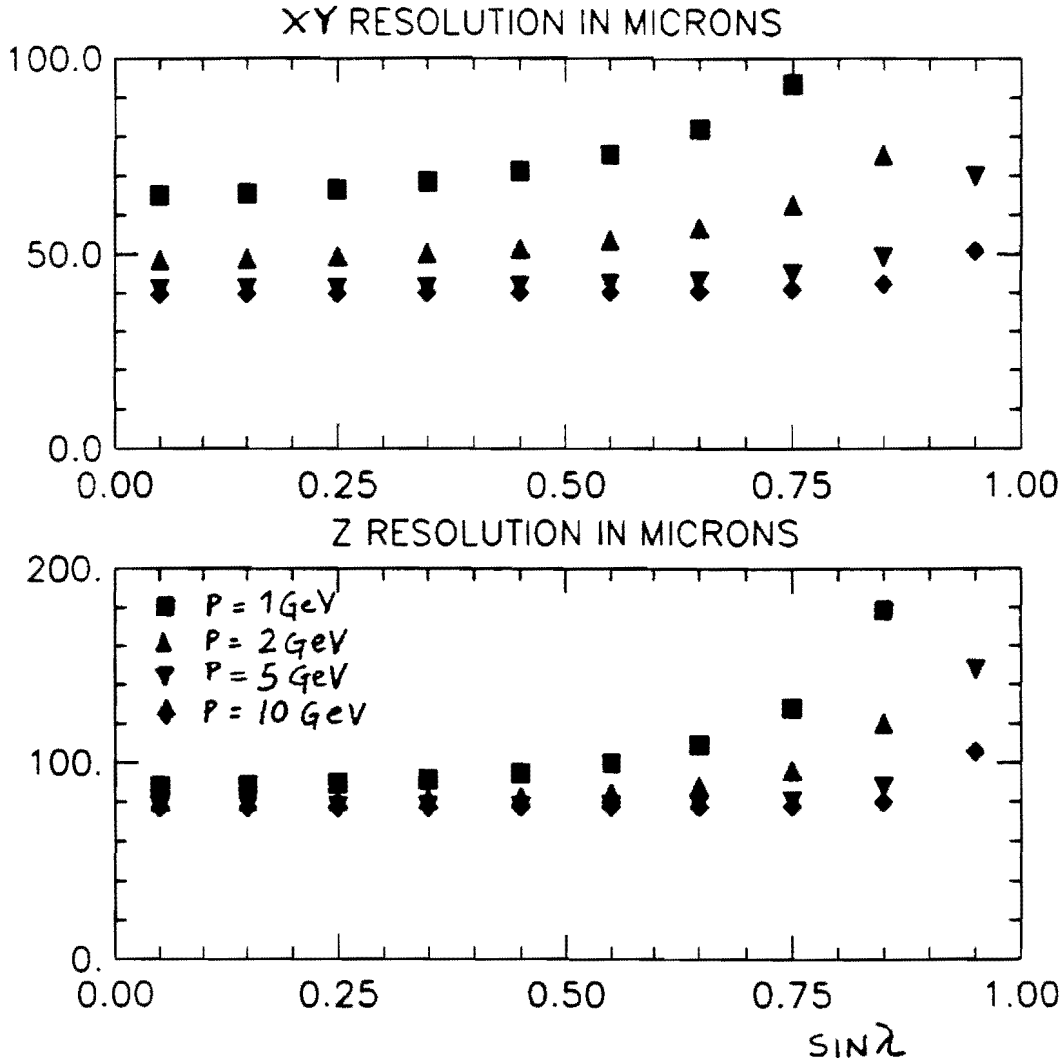

Figure 8: Impact parameter resolution of 1 layer double sided Silicon strip and 2 layer pixel detector as a function of the dip angle.

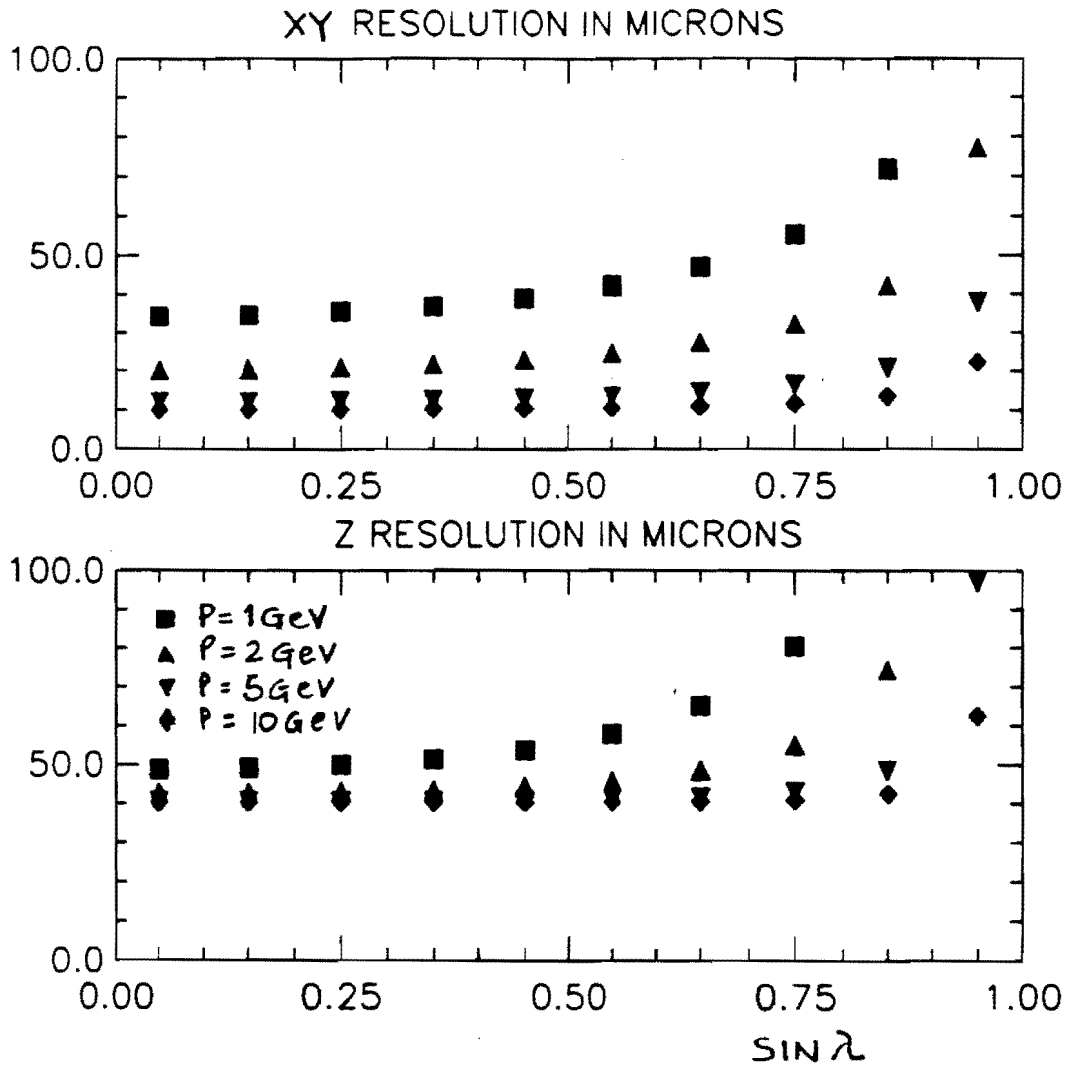

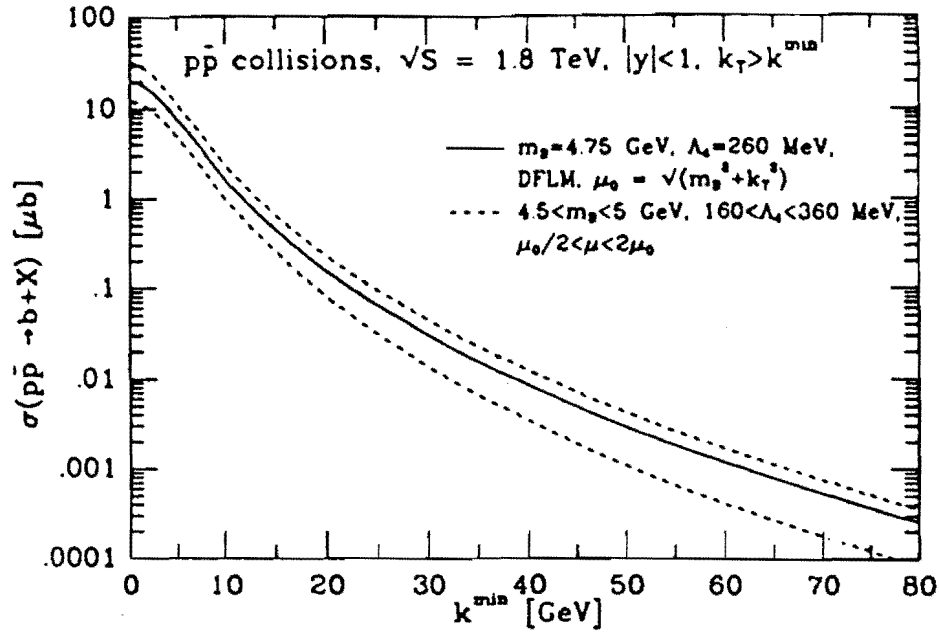

Fig. 9. Inclusive cross section for the production of a heavy quark with a mass of 4.75 GeV, with k_T and rapidity cuts at $\sqrt{S} = 1.8$ TeV.

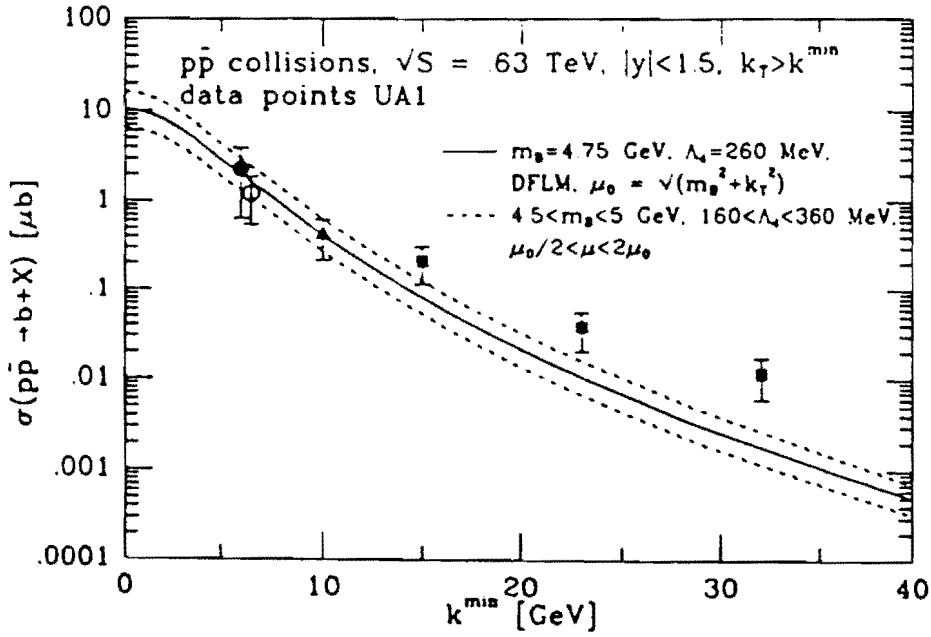

Fig. 10. Inclusive cross section for the production of a heavy quark with a mass of 4.75 GeV, with k_T and rapidity cuts, together with the corresponding experimental points from the UA1 experiment

Figure 11: Contours in cross-section for having both a $B^0 \to \psi K_S^0$ and a lepton from the other B with P_t values larger than those shown on the axes. The decay products of the B^0 and the lepton are required to be within $|\Delta y| < 2$.

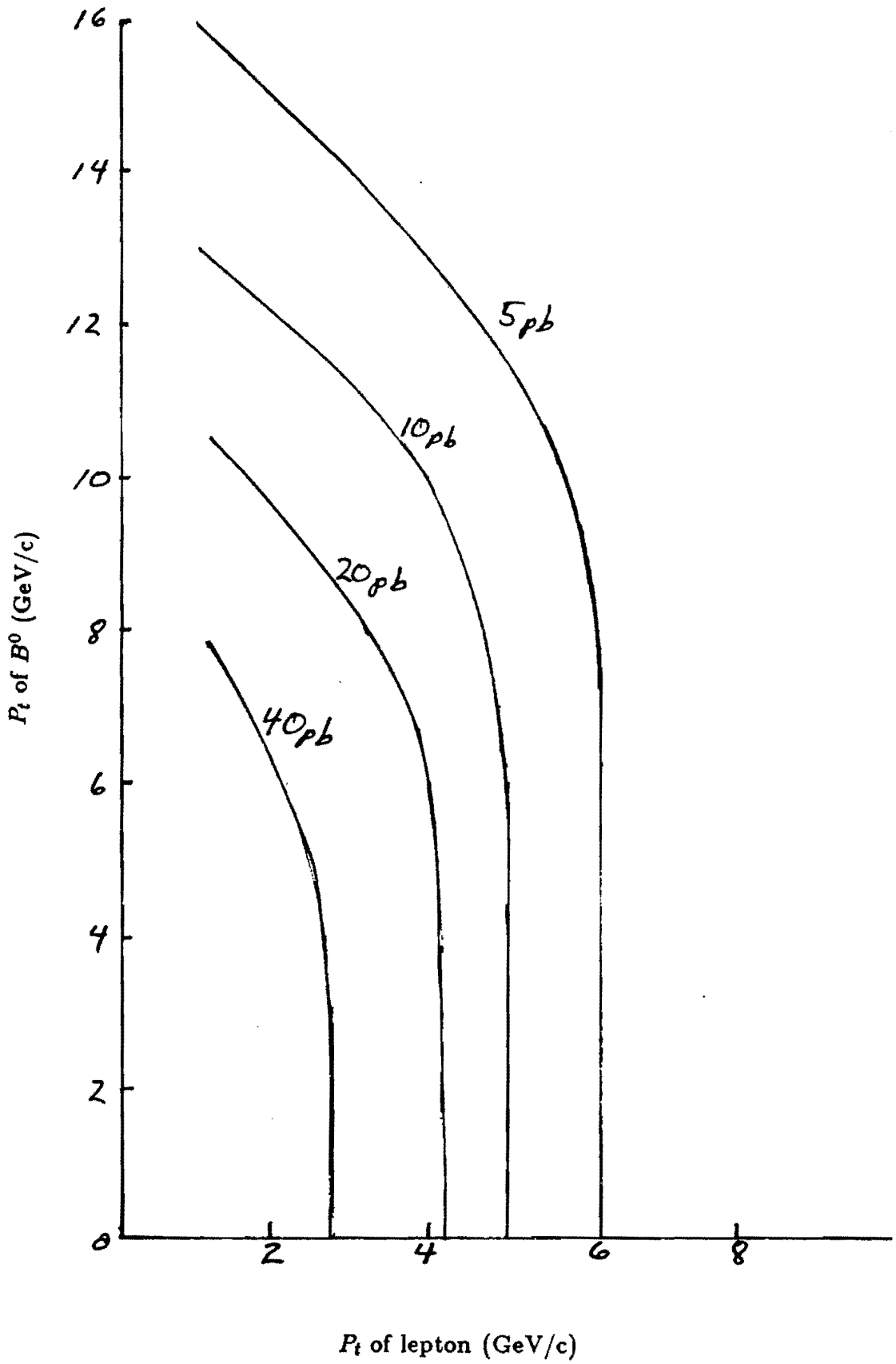
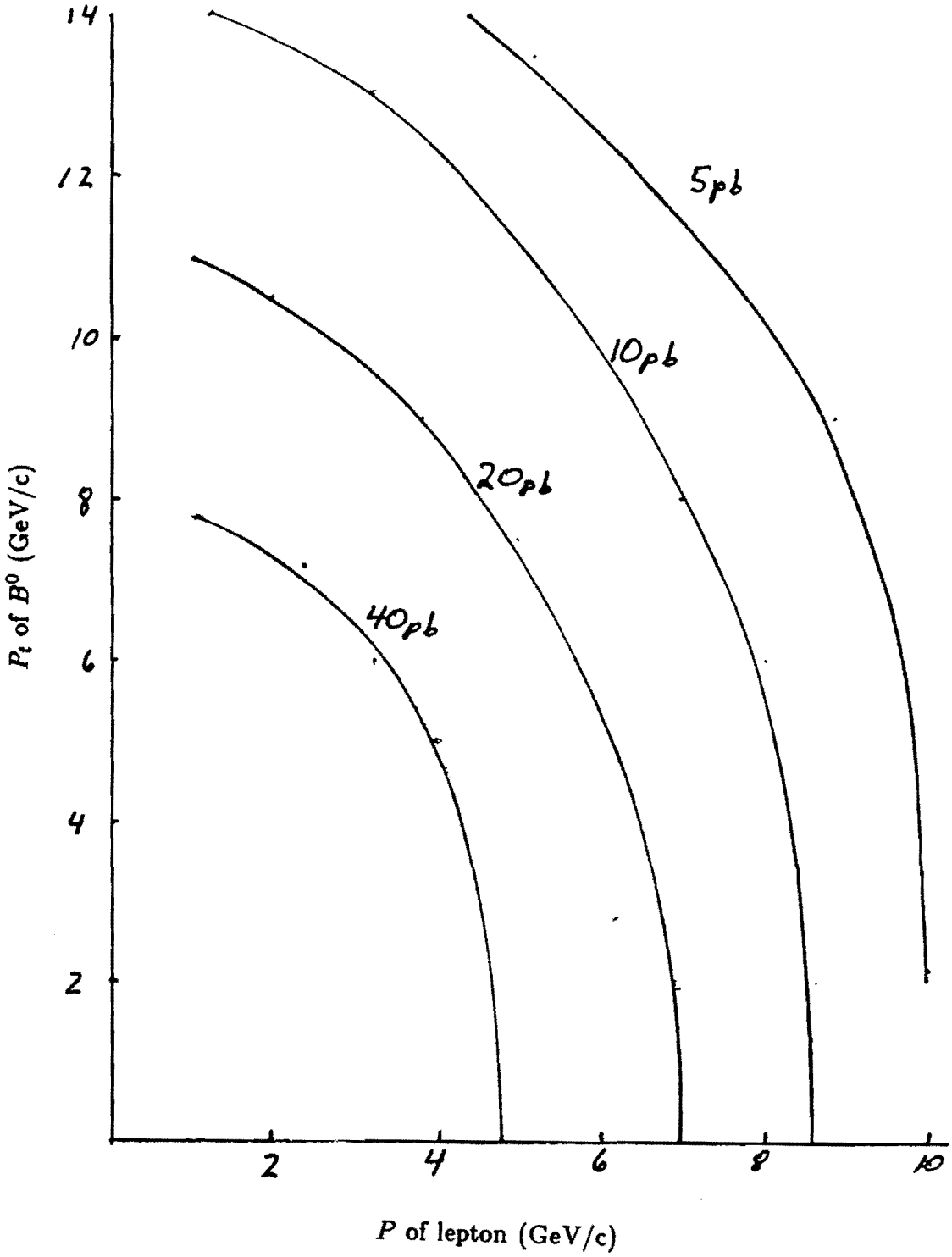
Figure 12: Contours in cross-section for having a $B^0 \rightarrow \psi K_S^0$ having a P_t value larger than that given on the vertical axis and and a lepton with P value larger than that given on the x axis.The decay products of the B^0 and the lepton are required to be within $|\Delta y| < 2$.